Dispersed Forces from Measured Shape Anisotropy of Adatom Islands: Revelations from an Accelerated Simulation Scheme

Frits Rabbering,[1] Abdelkader Kara,[2] Herbert Wormeester,[1,*] Teun Warnaar,[1] Oleg Trushin,[3] Talat. S. Rahman,[2] and Bene Poelsema[1]

[1]*MESA+ Institute for Nanotechnology, University of Twente, Enschede, The Netherlands*
[2]*Department of Physics, University of Central Florida, Orlando, Florida 32816, USA*
[3]*Institute of Microelectronics and Informatics, Academy of Sciences of Russia, Yaroslavl 150007, Russia*

(Received 11 May 2009; published 27 August 2009)

High resolution diffraction measurements reveal the emergence of anisotropic adatom islands during submonolayer homoepitaxial growth of Cu(001) at grazing incidence. This anisotropy is mimicked well in simulations only after the incorporation of attractive dipolar interactions between the surface and the atoms in the gas phase. The anisotropy of the islands depends markedly on the range of the attractive potential, which allows quantitative insight into the shape of the potential. The role of long- and short-ranged interactions is delineated.

DOI: 10.1103/PhysRevLett.103.096105 PACS numbers: 68.55.A−, 68.43.Hn, 77.22.Ej, 81.10.Aj

Nanopatterning has evolved into a vast area of research in which both top-down–bottom-up and combined top-down–bottom-up approaches are used. Exploitation of the growth kinetics in self-organization is a quite widely used bottom-up approach for the creation of patterns of dots or lines with high symmetry [1]. A sufficient bond between substrate and deposited materials imposes the symmetry of the substrate onto the grown pattern, resulting in triangular or hexagonal, square, and rectangular islands grown on fcc (111), (100), and (110) surfaces, respectively. Oblique incidence deposition can break this symmetry superimposed by the substrate, as, for instance, observed in magnetic properties [2,3]. This deposition angle related characteristic is exploited in many films of technological relevance and has led to the growth of layers with novel optical properties [4,5].

Homoepitaxial growth provides a suitable research area to investigate the influence of grazing angle deposition on symmetry and morphology. In a seminal series of experiments, van Dijken *et al.* [6,7] showed that the deposition of Cu on Cu(001) results in a breaking of the fourfold symmetry in submonolayer growth. They explained these results with the steering effect: attractive forces between an incoming atom and the substrate lead to deviations of the trajectory of the atom from a straight line. Protrusions or indentations on the surface modulate the actual arrival position with respect to the point of impact estimated from a long distance extrapolation. The result is a heterogeneous flux distribution and the growth of elongated adatom islands oriented perpendicular to the plane of incidence. Steering and the sequential diffusion dynamics at the very surface were evaluated theoretically by Montalenti and Voter for Ag(001) homoepitaxial growth [8]. Their accelerated molecular dynamics approach shows that at normal incidence up to temperatures of 70 K the interaction range is limited to 5 Å. Amar and co-workers [9–12] argued that the attractive interaction should be divided into short- and long-range parts, respectively, related to electron overlap interaction and dipole-dipole interaction. Via trajectory simulations near a step edge, they also concluded that at normal incidence only short-range interactions are important [9] and that it leads to a significant up-funneling in the deposition process. Calculations and experiments show that long-range steering effects are important for off-normal deposition angles above 50° [7,10]. Amar [10] has argued that the dipolar long-range interaction is overestimated by the Lennard-Jones (LJ) potential of Sanders and DePristo [13] that has been used in growth simulations by Seo *et al.* [14] and Montalenti *et al.* [8]. In general such questions can only be answered through simulations capable of incorporating microscopic features into predicting properties at scales of experimental relevance. In this Letter we show that while standard molecular dynamics (MD) and kinetic Monte Carlo (KMC) simulations have their own limitations, they can conspire to provide an accelerated scheme for accurately describing epitaxial growth. To make explicit the working of this scheme and the insights that it provides, we turn to the variation of the shape anisotropy of Cu adatom islands with submololayer coverage on Cu(001).

Homoepitaxial growth experiments on a Cu(001) surface held at 250 K were conducted in ultrahigh vacuum (base pressure $<10^{-10}$ mbar). Cu was deposited at a rate of 0.25 ML/min at a grazing angle of incidence (80° from the normal) along the [110] azimuth. The morphology was analyzed with high resolution low energy electron diffraction (HRLEED) after quickly cooling the sample to 100 K in order to freeze the morphology.

Figure 1 shows a measured diffraction image similar to the one reported by van Dijken *et al.* [6,7] after deposition of 0.5 ML at grazing incidence angle of 80° and $T = 250$ K with a deposition rate of 0.25 ML/min. For a

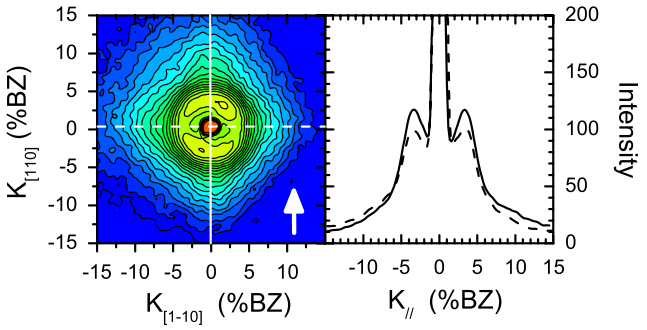

FIG. 1 (color online). Left-hand side: HRLEED image after 0.5 ML grown at a polar angle of incidence of 80° at $T = 250$ K with a rate $R = 0.25$ ML/min. The arrow indicates the deposition direction. Right-hand side: Line scans in the diffraction image parallel (solid line) and perpendicular (dashed line) to the deposition plane.

quantitative evaluation, the line scans in the two high symmetry directions are used (Fig. 1, right-hand side). The line scans parallel and perpendicular to the plane of incidence differ only by the intensity of the first maximum, $I_{[110]}$ and $I_{[\bar{1}10]}$, respectively. The similar position and width indicate the average distances L, and the stochastic variations of the distance in the [110] and the $[\bar{1}10]$ direction are identical. As a matter of fact, this comes as no surprise because of the isotropic diffusion on the Cu(001) surface. Fraunhofer diffraction describes the observed intensity profile [15], and the intensity at the first maximum in a high symmetry direction is proportional to $\sin^2(\pi W/L)/(W/L)^2$, with W the island width in that direction. For small shape anisotropy, it can be deduced that the intensity ratio at the first maximum as a function of coverage $\theta = (W_{[\bar{1}10]}W_{[110]})/L^2$ is [16]

$$\frac{I_{[\bar{1}10]}}{I_{[110]}} = (W_{[110]}/W_{[\bar{1}10]})^2 \frac{\sin^2(W_{[\bar{1}10]}/L)}{\sin^2(W_{[110]}/L)} \approx 1 + 2\left(1 + \frac{W_{[\bar{1}10]}}{W_{[110]}}\right)\left(1 - \frac{\pi\sqrt{\theta}}{\tan(\pi\sqrt{\theta})}\right). \quad (1)$$

The shape anisotropy depicted in Fig. 1 is about 1.9% and is the result of the steering effect, i.e., a heterogeneity in the trajectory of incident atoms.

To study quantitatively the influence of an adatom island on deposition trajectories we performed MD simulations with a simulated substrate temperature of 250 K. The interaction potential used in these MD simulations is a standard embedded atom method (EAM) potential [17] which was shown to describe accurately several surface and bulk properties of copper [18]. The MD cell used consists of a substrate of 8 Cu(001) layers of 20×6 atoms and an adatom island of 6×6 atoms. Periodic boundary conditions were applied parallel to the surface. This implies that the island resembles an infinitely long stripe of 6 atoms wide with an up and down step in the [110] direction parallel to the deposition plane. There is no periodic boundary in the vertical direction. Artifacts due to finite size effects are suppressed by partitioning the substrate in the vertical direction [17,19]. The lowest 2 layers are kept at fixed position to avoid global motion. The next three layers are held at constant temperature. These so-called sandbag layers absorb the excess energy introduced by the impinging atoms. The top 3 layers and the adatom island follow microcanonical dynamics. The incoming atoms have an initial velocity of 551 m/s equivalent to a kinetic energy of 0.1 eV and a far field polar deposition angle of 80° and are launched 5 Å above the average vertical position of the adatom island. One MD simulation of a deposition event results in the condensation of the incoming atom at one of the fourfold hollow sites on the surface. These condensation sites are labeled by 1–19 in Fig. 2, depending on their position perpendicular to the 6-atom wide stripe. A "no residence" region is located near the steps, occupied by half an atom from the adatom layer. This implies that without any interaction (no attraction and rigid lattice) the condensation sites 3 and 9 will receive 50% more flux at normal incidence deposition. In the x direction of the cell, i.e., in the plane of incidence, 400 equidistant starting points were chosen, while perpendicular to this (y direction), another 11 starting points distributed over half an atom width were chosen. We found that the atomic corrugation has only a minor influence.

Figure 3(a) shows results of the MD simulations for a polar angle of incidence of 80° at a temperature of 250 K. A standard EAM potential for Cu was used. The flux was normalized by the number of incident trajectories on a flat surface. The flux heterogeneity as a result of the attractive interaction is limited to the condensation position 4 at the up step and 9–12 for the down step. This flux distribution is only partly different from the situation without any attractive interaction on the incoming particle, i.e., shadow growth. In this latter case, an increase of the flux is found just in front of the step, i.e., in box 3. The interaction thus leads to an up-funneling current with a larger deposition flux on top of the adatom island, i.e., in box 4, as was also found previously [9]. The attractive interaction results in an

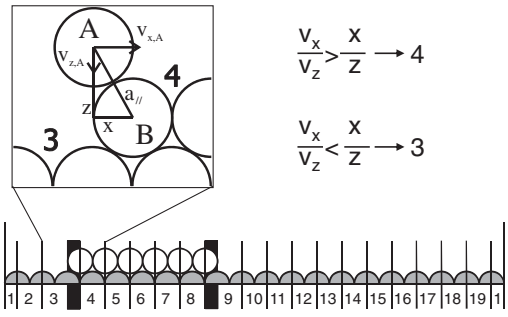

FIG. 2. Top: Illustration of the condensation rule for the incoming atom A as it gets into contact with a step edge atom B. Bottom: The substrate surface and an adatom island used in the trajectory calculations. Indicated are the condensation boxes 1–19 (see text). The black areas refer to nonresidence sites.

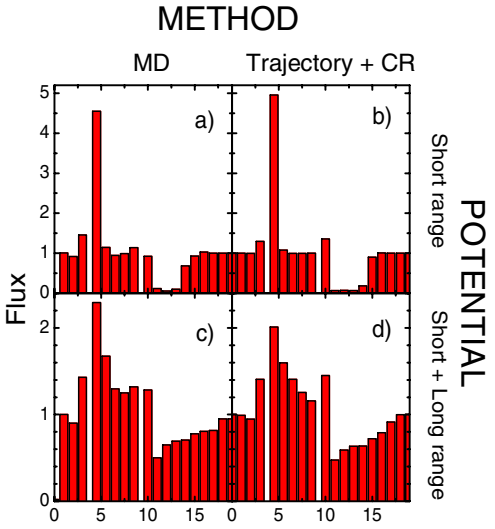

FIG. 3 (color online). Normalized heterogeneous flux on a substrate with an adatom island obtained for atoms incident from left to right at a far field polar angle of incidence of 80° evaluated. A full MD simulation with an EAM potential is compared to a calculation on a rigid lattice with a CR (see text). (a) EAM potential with only short-range interaction, (b) ϕ_{SR}, (c) EAM potential with extended interaction, (d) ϕ_{SDP}.

amount of flux in front of the island, box 3, of about 1.5. This amount is also found for normal incidence, and we found that it is virtually independent of the incidence angle. The total amount of extra material deposited on top of the adatom island equals the amount that is not deposited on the positions 9–12. The influence of the long-range dipolar interaction was incorporated in these MD calculations by adding a r^{-6} tail beyond the cutoff distance to the pair-pair potential with the strength of the LJ potential of Sanders and DePristo [13]; see Fig. 3(c). The amount of material "transferred" from behind the adatom island to on top is similar, but the distribution both on top and in the shadow region has markedly changed. Transient mobility effects were not observed in these MD simulations. Note that the very enhancement of the flux on top of the islands is responsible for the shape anisotropy of the adatom islands [3,6,7].

A full molecular dynamic simulation of trajectories of incoming atoms is too time-consuming to describe growth at realistic substrate temperatures, deposition fluxes, and time scales. Therefore, a condensation rule (CR) that efficiently determines the position of accommodation on a frozen surface is urgently required. The MD simulations show that the condensation process is quite subtle and requires specific attention. The determination of the condensation site for the CR is illustrated in Fig. 2 for an atom arriving near a step atom. A natural choice is to compare the velocity direction $[(v_x/v_z)]$ with the direction of the center line between the incoming atom and the nearest (substrate) atom $[(x/z)]$, upon impact in the rigid lattice geometry. An up-funneling event occurs (condensation in capture zone 4 in Fig. 2) if the velocity direction is larger than the direction of the center line $[(v_x/v_z) > (x/z)]$. Otherwise, the atom shows down-funneling (condensation in capture zone 3). The Sanders and DePristo attractive pair-pair potential ϕ_{SDP} was used to verify the accuracy of this concept:

$$\phi_{\mathrm{SDP}}(r) = \frac{c_{12}}{r^{12}} - \frac{c_6}{r^6}, \tag{2}$$

with $c_{12} = 36.7$ keV/Å^{10} and $c_6 = 242$ eV/Å^6. These parameters were derived from the nearest neighbor distance and the condensation energy and provide an interaction very similar to the EAM potential. A short-range potential ϕ_{SR} is obtained using an appropriate cutoff function:

$$\phi_{\mathrm{SR}} = \phi_{\mathrm{SDP}} \frac{(r^2 - r_c^2)^2}{(r^2 - r_c^2)^2 + Q^2}, \qquad r \le r_c;$$
$$\phi_{\mathrm{SR}} = 0, \qquad r > r_c. \tag{3}$$

The results shown in Fig. 3(b) are for $r_c = 7$ Å and $Q = 0.65$ Å^2. Figures 3(b) and 3(d) show that the condensation rule applied to the rigid lattice suffice to evaluate condensation positions similar to a full MD calculation.

The long-range dipolar interaction is provided by the r^{-6} term in the pair-pair potential. However, as argued by Amar [10], ϕ_{SDP} overestimates the actual strength in the dipolar range. Based on the optical properties of the materials an about 5 times smaller dipolar interaction has been evaluated. A reduced long-range interaction can be incorporated by a modification of the pair-pair potential:

$$\phi_M(r) = \frac{c_{10}}{r^{10}} - \frac{c_8}{r^8} - \frac{c_6}{r^6}, \tag{4}$$

with $c_{10} = 21.9$ keV/Å^{10}, $c_8 = 3.85$ keV/Å^8, and $c_6 = 47.1$ eV/Å^6. This potential gives the same condensation

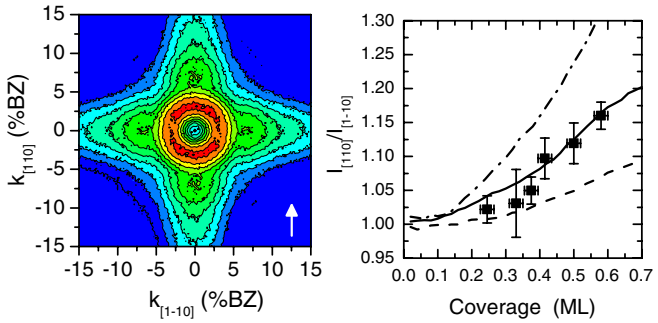

FIG. 4 (color online). Left-hand side: Contour plot of the calculated diffraction image after deposition of 60% ML averaged over 128 simulations at grazing incidence of 80° at a temperature of 250 K at deposition rate of 0.6 ML/min. The simulation has been carried out with the ϕ_M potential. The arrow indicates the deposition direction. Right-hand side: Intensity anisotropy in the diffraction image as a function of coverage as measured (■) and calculated for the standard potential ϕ_{SDP} (dashed line), the modified potential ϕ_M (solid line), and for short-range interaction ϕ_{SR} (dash-dotted line).

energy and nearest neighbor distance as ϕ_{SDP}, but the c_6 value is reduced by a factor of 5.

The efficient trajectory calculations have been incorporated in a KMC scheme that describes the diffusion processes. The intralayer mass transport was modeled using the energy barriers given by Biham *et al.* [20]. The interlayer mass transport is almost exclusively via kink positions on this surface [21]. An additional energy barrier of -3 meV for these kinks provides a growth with roughness and characteristic length scales that are very similar to experimentally observed values after normal incidence growth in a wide temperature range [22]. The simulations presented in this work were performed on a grid of 512×512 atoms^2 with periodic boundary conditions.

The simulation results were compared with experiments by calculating the diffraction image of the simulated morphology at an out-of-phase condition. A diffraction image at 0.5 ML coverage obtained with the modified interaction potential is shown in Fig. 4(a). The change in anisotropy with coverage was evaluated for the three interaction potentials. The results of these simulations are shown in Fig. 4(b) as well as experimental results determined from HRLEED as a function of coverage. A very different evolution of the diffraction intensity anisotropy is observed for the three interaction potentials. Surprisingly, the short-range potential clearly overestimates the experimentally found anisotropy. The ϕ_{SDP} potential, on the other hand, underestimates the effect for higher coverages. The modified potential describes the experimental results quite well. Both in the present experiments as well in previous experiments [6,7], an intensity ratio of about 15% was measured around 0.5 ML coverage. This value corresponds to that obtained with the modified potential. The coverage range is limited to about 0.6 ML. Above this coverage the azimuthal ordering of the islands changes to a checkerboardlike pattern that complicates the determination of the anisotropy. Also, strong progressing coalescence prevents the use of higher coverages. The difference in the anisotropy for the three interaction potentials can be explained from Figs. 3(b) and 3(d). The short-range interaction leads to the large flux enhancement on top of adatom islands and is already effective for small structures. The dipolar interaction has great influence on the distribution over the island and results in a less efficient up-funneling for smaller structures, i.e., in the low coverage regime.

In conclusion, we have shown that for grazing incidence deposition both the long- and short-range attractive interaction between the incoming particle and the actually growing surface have important consequences for the steering effect. We have defined a condensation rule that determines the accommodation position on the surface of an incoming atom. The use of this condensation rule allows a reliable calculation of the flux distribution due to steering as shown by comparison with MD calculations. Trajectory calculations and a KMC algorithm for diffusion processes on the Cu(001) surfaces result in the observation of rectangular islands with their long axis perpendicular to the deposition plane, similar to experimental results obtained for submonolayer coverage. The pronounced sensitivity of the obtained island shape anisotropy for the applied interaction potential opens a powerful way to gain insight in the shape of the attractive potential. A modified LJ potential, which also accounts properly for the optical properties of Cu, yields results that lead to a convincing quantitative agreement with experimental data in the entire coverage regime.

This work is part of the research program of the Stichting Fundamenteel Onderzoek der Materie (FOM), financially supported by the Nederlandse Organisatie voor Wetenschappelijk Onderzoek (NWO). The work of A. K. and T. S. R. was supported by NSF-USA under Grant No. ITR-0428826.

*Corresponding author.
h.wormeester@utwente.nl

[1] H. Brune, Surf. Sci. Rep. **31**, 125 (1998).
[2] S. van Dijken, G. Di Santo, and B. Poelsema, Appl. Phys. Lett. **77**, 2030 (2000).
[3] A. Lisfi, J. C. Lodder, H. Wormeester, and B. Poelsema, Phys. Rev. B **66**, 174420 (2002).
[4] G. Beydaghyan, K. Kaminska, T. Brown, and K. Robbie, Appl. Opt. **43**, 5343 (2004).
[5] H. E. Ruda *et al.*, Nanoscale Res. Lett. **1**, 99 (2006).
[6] S. van Dijken, L. C. Jorritsma, and B. Poelsema, Phys. Rev. Lett. **82**, 4038 (1999).
[7] S. van Dijken, L. C. Jorritsma, and B. Poelsema, Phys. Rev. B **61**, 14 047 (2000).
[8] F. Montalenti and A. F. Voter, Phys. Rev. B **64**, 081401 (2001).
[9] J. G. Yu and J. G. Amar, Phys. Rev. Lett. **89**, 286103 (2002).
[10] J. G. Amar, Phys. Rev. B **67**, 165425 (2003).
[11] J. G. Yu, J. G. Amar, and A. Bogicevic, Phys. Rev. B **69**, 113406 (2004).
[12] J. G. Yu and J. G. Amar, Phys. Rev. B **69**, 045426 (2004).
[13] D. E. Sanders and A. E. DePristo, Surf. Sci. **254**, 341 (1991).
[14] J. Seo, S. M. Kwon, H. Y. Kim, and J. S. Kim, Phys. Rev. B **67**, 121402 (2003).
[15] E. Hecht and A. Zajac, *Optics* (Addison-Wesley, Reading, MA, 1974).
[16] F. L. W. Rabbering, Ph.D. thesis, University of Twente, 2008.
[17] M. S. Daw, S. M. Foiles, and M. I. Baskes, Mater. Sci. Rep. **9**, 251 (1993).
[18] A. Kara and T. Rahman, Surf. Sci. Rep. **56**, 159 (2005).
[19] S. M. Foiles, M. I. Baskes, and M. S. Daw, Phys. Rev. B **33**, 7983 (1986).
[20] O. Biham, I. Furman, M. Karimi, G. Vidali, R. Kennett, and H. Zeng, Surf. Sci. **400**, 29 (1998).
[21] M. Li, J. F. Wendelken, B.-G. Liu, E. G. Wang, and Z. Zhang, Phys. Rev. Lett. **86**, 2345 (2001).
[22] F. L. W. Rabbering, H. Wormeester, F. Everts, and B. Poelsema, Phys. Rev. B **79**, 075402 (2009).